Bond Breaking in the Chemical Vapor Deposition Precursor (1,1,1,5,5,5-Hexafluoro-2,4-pentanedionato)(η^2-1,5-cyclooctadiene)-copper(I) Studied by Variable-Temperature X-ray Crystallography and Solid-State NMR Spectroscopy[1]

Ravi Kumar, Frank R. Fronczek, Andrew W. Maverick,* Ae Ja Kim, and Leslie G. Butler*

Department of Chemistry, Louisiana State University, Baton Rouge, Louisiana 70803

Received September 13, 1993. Revised Manuscript Received February 7, 1994®

Bond breaking in chemical vapor deposition (CVD) and fluxional processes in the solid state depend on the same fundamental molecular properties, and cross-fertilization between these two separate areas is attempted herein. X-ray crystallograpic and solid-state NMR studies of (hfac)Cu^{I}(COD) (hfac = 1,1,1,5,5,5-hexafluoro-2,4-pentanedione; COD = 1,5-cyclooctadiene) reveal that the Cu atom is disordered between two sites. The two disordered molecules (represented by the disordered atoms Cu and Cu′) are crystallographically inequivalent, but they have the same connectivity, with η^2 coordination of Cu to the COD ligand (in contrast to our previous proposal of η^2 and η^4 sites in equilbrium: Kumar, R.; et al. *Chem. Mater.* **1992**, *4*, 577). X-ray structural data recorded at three temperatures lead to estimates of the relative populations of Cu and Cu′, which correspond to an energy difference of 3–5 kJ mol^{-1}. ($CuC_{13}H_{13}F_6O_2$, monoclinic, space group $P2_1/c$; $Z = 4$. At 195 K, $a = 9.980(5)$, $b = 9.690(2)$, $c = 15.547(7)$ Å; $\beta = 107.31(2)°$, $R = 0.044$ and $R_w = 0.056$ for 4517 reflections and 256 parameters; populations Cu:Cu′ = 0.944:0.056. At 110 K, $a = 9.917(5)$, $b = 9.583(2)$, $c = 15.452(7)$ Å; $\beta = 106.69(4)$; $R = 0.034$ and $R_w = 0.039$ for 3524 reflections and 255 parameters; populations 0.990:0.010.) ^{13}C CP/MAS spectra show increasingly rapid interconversion between the two sites at higher temperatures, with two separate resonances at 127 and 105 ppm (free and bound —*C*H= sites in the same COD ligand) coalescing into a single resonance at 340 K. Line-shape analysis yields an interconversion barrier of ca. 60 kJ mol^{-1}. This barrier is similar to previously reported experimental activation barriers for dissociation of olefins from Cu surfaces or from Cu(I) complexes adsorbed on Cu surfaces, suggesting that the Cu–olefin bond may be nearly broken in the transition state for the Cu ↔ Cu′ interconversion.

Introduction

Copper(I) β-diketonate complexes have received increasing attention in recent years. In the first systematic study, in 1985, of (hfac)Cu^{I}(olefin)[2a] and related complexes, Doyle and co-workers reported that several of the complexes were volatile and could be induced to decompose into Cu metal.[2b] Since that time, several research groups have used the complexes as precursors for chemical vapor deposition (CVD) of copper metal, via either H_2 reduction (eq 1)[3] or disproportionation (eq 2).[4-7] The mechanism of

$$(\text{hfac})\text{Cu}^{I}(\text{COD}) + {}^1/_2\text{H}_2 \rightarrow \text{Cu(s)} + \text{hfacH(g)} + \text{COD(g)} \quad (1)$$

$$2(\text{hfac})\text{Cu}^{I}(\text{COD}) \rightarrow \text{Cu(s)} + \text{Cu}^{II}(\text{hfac})_2\text{(g)} + 2\text{COD(g)} \quad (2)$$

the disproportionation process (eq 2) on metal surfaces is believed to involve initial rapid dissociation of COD. Two of the remaining (hfac)Cu moieties then react further to produce one gaseous Cu^{II}(hfac)$_2$ molecule and one Cu atom.[8] The activation energy for the dissociation of COD under these conditions has been reported to be 59 kJ mol^{-1}.[9] We now report a study of structure and dynamics in crystalline (hfac)Cu^{I}(COD) (Figure 1) which suggests a similar barrier (ca. 60 kJ mol^{-1}) for reversible dissociation of the COD ligand in the crystalline environment.

Our initial report of Cu CVD via H_2 reduction of (hfac)-Cu(COD) included an analysis of the crystal structure of the precursor at room temperature. We proposed that this solid contains primarily (hfac)Cu(η^2-COD), with the 18-electron (hfac)Cu(η^4-COD) isomer present in smaller

* Abstract published in *Advance ACS Abstracts*, April 1, 1994.

(1) Reported in part at the 205th National Meeting of the American Chemical Society, Denver, CO; April 1993; Abstract No. 92, INOR; and at the Annual Meeting of the American Crystallographic Association, Albuquerque, NM, May 1993; Abstract No. PC03.

(2) (a) Abbreviations: CP/MAS = cross polarization/magic angle spinning; hfacH = 1,1,1,5,5,5-hexafluoro-2,4-pentanedione; COD = 1,5-cyclooctadiene; COT = 1,3,5,7-cyclooctatetraene; tmvs = trimethylvinylsilane; Cy_3P = tricyclohexylphosphine; amp = 2-(aminomethyl)-pyridine; $TPPH_2$ = tetraphenylporphyrin. (b) Doyle, G.; Eriksen, K. A.; Van Engen, D. *Organometallics* **1985**, *4*, 830.

(3) Kumar, R.; Fronczek, F. R.; Maverick, A. W.; Lai, W. G.; Griffin, G. L. *Chem. Mater.* **1992**, *4*, 577.

(4) Hampden-Smith, M. J.; Kodas, T. T. In *Chemistry of Chemical Vapor Deposition*; Kodas, T. T., Hampden-Smith, M. J., Eds.; VCH: Weinheim, in press; Chapter 5, and references therein.

(5) Jain, A.; Chi, K. M.; Hampden-Smith, M. J.; Kodas, T. T.; Farr, J. D.; Paffett, M. *J. Mater. Res.* **1992**, *7*, 261.

(6) Reynolds, S. K.; Smart, C. J.; Baran, E. F.; Baum, T. H.; Larson, C. E.; Brock, P. J. *Appl. Phys. Lett.* **1991**, *59*, 2332.

(7) Norman, J. A. T.; Muratore, B. A.; Dyer, P. N.; Roberts, D. A.; Hochberg, A. K.; Dubois, L. H. *Mater. Sci. Eng.* **1993**, *B17*, 87.

(8) Cohen, S. L.; Liehr, M.; Kasi, S. *J. Vac. Sci. Technol. A* **1992**, *10*, 863.

(9) Dubois, L. H.; Zegarski, B. R. *J. Electrochem. Soc.* **1992**, *139*, 3295.

0897-4756/94/2806-0587$04.50/0

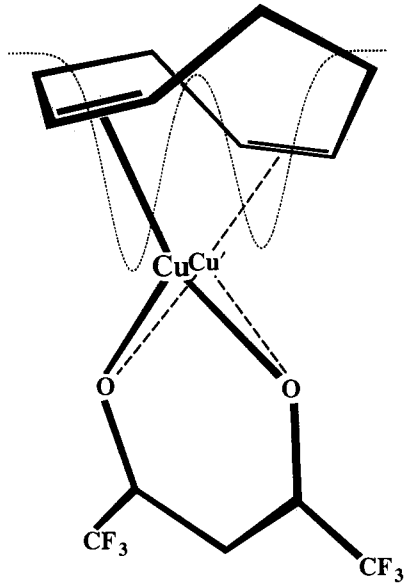

Figure 1. Schematic drawing of disorder model for crystalline (hfac)Cu^{I}(COD). Atom labeled Cu is bound to double bond in foreground ("η^{2}"); Cu' is bound to double bond in background ("$\eta^{2'}$"). Curve represents a possible potential-energy diagram for the Cu ↔ Cu' interconversion.

amounts. (The existence of well-defined groups of complexes containing (hfac)Cu bound to one or two additional ligands (e.g., hfac)CuL$_n$, L = phosphine, alkyne; n = 1, 2)[10,11] suggests that 16- and 18-electron Cu(I) species can have similar stability.) We have now collected higher-resolution single-crystal X-ray data for (hfac)Cu(COD) at two lower temperatures, rerefined the structure using the room-temperature data set, and compared these results with the X-ray study of Hampden-Smith and co-workers;[12] we have also carried out a solid-state ^{13}C CP/MAS study of the solid as a function of temperature.

Variable-temperature solid-state ^{13}C CP/MAS (cross polarization/magic angle spinning) NMR combined with X-ray crystallographic studies yield great insight into solid-state structure and dynamics. An early application of this combination of techniques was to solid-state tautomerization of the hydroxy ketone naphthazarin B.[13] Other applications have included the problem of the nonclassical carbonium ion in the 2-norbornyl cation and "ring whizzing" in pentacarbonyl(cyclooctatetraene)diiron[14] and, more recently, C_{60} and related compounds[15] and organotin polymers.[16]

The new X-ray data presented here for (hfac)Cu(COD) provide no convincing evidence in favor of the η^{4}-COD structure. Instead, X-ray and NMR data are best explained by two crystallographically inequivalent η^{2}-COD sites whose relative populations and interconversion rates vary with temperature. Analysis of the populations of the two sites suggests that they differ in energy by 3–5 kJ mol^{-1}. The barrier to interconversion between the two Cu sites is ca. 60 kJ mol^{-1}, as deduced from the solid-state NMR data. The barrier is similar to experimental activation barriers reported for two other processes that involve breaking of copper–olefin bonds: dissociation of COD from (hfac)Cu(COD) adsorbed on copper (59 kJ mol^{-1})[9] and desorption of ethylene from copper (47 and 67 kJ mol^{-1}).[17]

Experimental Section

Materials. The complexes (hfac)CuL (L = 1,5-cyclooctadiene (COD) and cyclooctene) were prepared according to the literature procedure.[2b] The COD complex was purified by sublimation under N_2 at 85 °C. The resulting material, stored in a drybox under N_2, was satisfactory for NMR measurements. Single crystals for X-ray analysis were grown at ca. −5 °C by layering a solution of the purified complex in CH_2Cl_2 with hexane. $PdCl_2$(η^{4}-COD),[18] [Cu(η^{2}-NBD)]$_4$(μ_3-Cl)$_4$,[19] and [Cu(η^{4}-COD)]$_2$(μ-Cl)$_2$[20] were prepared by literature methods.

X-ray Analysis: Data Collection. Diffraction data were collected on an Enraf-Nonius CAD4 diffractometer fitted with Mo Kα source and graphite monochromator, using the θ–2θ scan method. Final unit-cell constants were determined from the orientations of 25 centered high-angle reflections. The intensities were corrected for absorption using ψ-scan data (five reflections measured for each data set). The crystals were cooled in a thermostated N_2 cold stream.

At 195 K, data collection was straightforward. At 110 K, however, many (hfac)Cu(COD) crystals cracked, especially if they were placed directly in the cold N_2 gas stream or had been cut from a larger crystal. The crystal chosen for data collection at 110 K was placed in the gas stream at ca. 240 K and then cooled to the desired temperature over a period of ca. $^1/_2$ h.

Refinement. Parameters for the new data sets and refinements are included in Table 1. In all of the present analysis, the atomic coordinates from our previous study[3] were used as the starting point, and the MolEN[21] set of programs was used. In each case, we attempted to refine the structure using three different assumptions concerning the occupancies at the Cu and Cu' sites: (1) refining the occupancies of both Cu and Cu' independently; (2) refining the occupancy of Cu and constraining the occupancy of Cu' to be equal to (1 − (occupancy of Cu)); (3) the reverse of (2), refining the occupancy of Cu' and applying the constraint to Cu. The results of these population analyses and their interpretation in terms of energy differences between the Cu and Cu' sites (see Discussion) are presented in Table 2.

(*a*) *Rerefinement Using Room-Temperature Data.* Refinement (1), in which no constraints were placed on the occupancies or the anisotropic displacement parameters for Cu or Cu', was successful: the occupancies converged to 0.7683 and 0.2201, respectively. Because the sum of these occupancies was not exactly 1, they were rescaled in proportion, to 0.777 35 and 0.222 65, respectively, and then fixed for the final stages of refinement. H atom positions were calculated, and their isotropic displacement parameters U_{iso} fixed at $1.3U_{eq}$ for the attached carbon atom. All non-hydrogen atoms, except the minor F atoms (F1'–F6') in the disordered CF_3 groups, were refined anisotropically. Refinements by methods (2) and (3) also converged (see Table 2), but they produced no changes in any coordinates or displacement parameters that were greater than their estimated standard deviations.

(10) Shin, H.-K.; Chi, K. M.; Farkas, J.; Hampden-Smith, M. J.; Kodas, T. T.; Duesler, E. N. *Inorg. Chem.* **1992**, *31*, 424.
(11) Shin, H.-K.; Hampden-Smith, M. J.; Duesler, E. N.; Kodas, T. T. *Can. J. Chem.* **1992**, *70*, 2954.
(12) Shin, H.-K.; Hampden-Smith, M. J.; Kodas, T. T.; Duesler, E. N. *Polyhedron* **1991**, *10*, 645.
(13) Shiau, W.-I.; Duesler, E. N.; Paul, I. C.; Curtin, D. Y.; Blann, W. G.; Fyfe, C. A. *J. Am. Chem. Soc.* **1980**, *102*, 4546–8. For a recent review of these and related approaches to studying the dynamics of organometallic solids, see: Braga, D. *Chem. Rev.* **1992**, *92*, 633.
(14) Lyerla, J. R.; Yannoni, C. S.; Fyfe, C. A. *Acc. Chem. Res.* **1982**, *15*, 208.
(15) Johnson, R. D.; Bethune, D. S.; Yannoni, C. S. *Acc. Chem. Res.* **1992**, *25*, 152.
(16) Kümmerlen, J.; Sebald, A. *J. Am. Chem. Soc.* **1993**, *115*, 1134.
(17) Jenks, C. J.; Bent, B. E.; Bernstein, N.; Zaera, F. *Surf. Sci.* **1992**, *277*, L89. Ertürk, Ü.; Otto, A. *Surf. Sci.* **1987**, *179*, 163.
(18) Chatt, J.; Vallarino, L. M.; Venanzi, L. M. *J. Chem. Soc.* **1957**, 3413.
(19) Baenziger, N. C.; Haight, H. L.; Doyle, J. R. *Inorg. Chem.* **1964**, *3*, 1535.
(20) van den Hende, J. H.; Baird, W. C., Jr. *J. Am. Chem. Soc.* **1963**, *85*, 1009.
(21) Fair, C. K. *MolEN. An Interactive Structure Solution Procedure*; Enraf-Nonius: Delft, The Netherlands, 1990.

Table 1. Data Collection and Refinement Parameters for (hfac)Cu(COD)[a]

	temp/K				
	296 ± 2[b]		243[c]	195 ± 3[d]	110 ± 3[d]
formula			$CuC_{13}H_{13}F_6O_2$		
formula wt			378.8		
color			yellow		
λ/Å			0.710 73 (Mo Kα)		
space group			$P2_1/c$		
Z			4		
habit	parallelepiped		prism	parallelepiped	parallelepiped
cryst dimens/mm	0.35 × 0.48 × 0.50		0.34 × 0.41 × 0.46	0.35 × 0.55 × 0.68	0.30 × 0.45 × 0.50
a/Å	10.042(2)		10.011(2)	9.980(5)	9.917(5)
b/Å	9.878(2)		9.777(3)	9.690(2)	9.583(2)
c/Å	15.756(3)		15.658(3)	15.547(7)	15.452(7)
β/deg	108.64(2)		107.88(2)	107.31(2)	106.69(4)
V/Å^3	1481(1)		1457.6(6)	1436(2)	1407(2)
ρ_x (ρ_m)/g cm^{-3}	1.699 (1.74(5))		1.726	1.753	1.789
μ/cm^{-1}	15.4		15.7	15.9	16.2
transm coeff	0.833–0.999		0.582–0.808	0.924–0.998	0.815–0.998
θ range/deg	1–25		1–25	1–38	1–32
scan type	ω–2θ		ω	ω–2θ	ω–2θ
octs collcd	$hk\pm l$		$\pm h\pm kl$	$hk\pm l$	$hk\pm l$
R_{INT}[e]	0.015		0.027	0.019	0.014
unique data	2604		2565	7755	4203
refls obsd	1790 ($I > 3\sigma(I)$)		1928 ($F > 3\sigma(F)$)	4517 ($I > 3\sigma(I)$)	3524 ($I > 3\sigma(I)$)
decay, std rf	4.4%			none	none
parameters	233[b]	233[d,f]	199	256	255
max shift/esd	0.09	0.05	<0.01	0.14	0.05
$R(F_o)$[g]	0.044	0.044	0.073	0.044	0.034
$R_w(F_o)$[h]	0.051	0.051	0.077	0.056	0.039
GOF[i]	2.65	2.65	1.87	2.72	2.40
max resid/e Å^{-3}	0.30	0.30	1.70	0.83	0.61
min resid/e Å^{-3}	−0.30	−0.30	−1.03	−0.20	−0.16
extinction[j]	6.93(5) × 10^{-6}	6.90(5) × 10^{-6}		1.59(6) × 10^{-6}	5.9(6) × 10^{-7}

[a] In Tables 1, 3, and 4, estimated standard deviations in the least significant digits of the values are given in parentheses. [b] Reference 3. [c] Reference 12. [d] This work. [e] Agreement factor on I for equivalent observed reflections. [f] Alternate refinement of data from ref 3 (see text for details). [g] $R = \sum||F_o| - |F_c||/\sum|F_o|$. [h] $R_w = \sqrt{(\sum w(|F_o| - |F_c|)^2/\sum wF_o^2)}$; $w = 4F_o^2/(\sigma^2(I) + (0.02F_o^2)^2)$ used for 296, 195, and 110 K structures. [i] GOF $= \sqrt{[\sum w(|F_o| - |F_c|)^2/(N_{obs} - N_{param})]}$. [j] Coefficient g in correction factor $(1 + gI_c)^{-1}$ applied to F_c.

Table 2. Energetics and Dynamics for the Disordered Copper Atom in (hfac)Cu(COD)

	X-ray occupancies (Cu, Cu′) and energetics						dynamics from NMR	
T/K	both refined	Cu refined	Cu′ refined	final value[a]	K_{eq}[a]	ΔG/kJ mol^{-1}	k/s^{-1}	$\Delta G^{\ddagger}$/kJ mol^{-1}
340							(5 ± 2) × 10^3	59.6 ± 1.2
320							(6 ± 3) × 10^2	61.5 ± 1.5
296	0.777, 0.223	0.769, 0.221	0.780, 0.220		0.2864	3.08	(2 ± 1) × 10^2 [b]	60.3 ± 1.4
195		0.933, 0.067	0.955, 0.045	0.944, 0.056	0.0593	4.58		
110		0.987, 0.013	0.993, 0.007	0.990, 0.010	0.0101	4.20		

[a] Determined from the values obtained when both Cu and Cu′ occupancies were refined (at 296 K) or from the average of the two sets of refined occupancies (195 and 110 K). These occupancies were then used to calculate K_{eq}. See text for details. [b] 300 K.

(*b*) *Using 195 and 110 K Data.* For both of these data sets, Cu′ was omitted in the early stages of the refinement. When this model converged, a difference Fourier map revealed a peak close to Cu, which we used as the initial location for Cu′. Refinement method (1) (refining independent occupancies and displacement parameters for both Cu and Cu′; see above) failed for both low-temperature data sets, apparently because the occupancy of Cu′ is low. However, methods (2) and (3) were successful. For the final refinements, the Cu and Cu′ occupancies were fixed at the averages of the refined values from methods (2) and (3). Only a single set of F atom coordinates was judged to be necessary in the 195 and 110 K models, in contrast to the room-temperature models, which included two disordered sets of F atoms. (The largest peaks in the final difference Fourier maps at both 195 and 110 K were ca. 1.25 Å from C4; we attribute these to some residual disorder in the CF_3 groups.)

195 K: The initial difference Fourier peak height corresponding to Cu′ was 3.7 e Å^{-3}. Cu′ could not be refined anisotropically. Cu′ and all H atoms were refined isotropically, and all other atoms were refined anisotropically. Depending on the refinement method (see above), the occupancies of Cu and Cu′ changed as outlined in Table 2, but no other parameters changed by more than 10% of their estimated standard deviations.

110 K: The initial difference Fourier peak height corresponding to Cu′ was 0.63 e Å^{-3}. Cu′ could not be refined anisotropically, nor could both occupancy and U_{iso} for Cu′ be refined simultaneously. Therefore, U_{iso} for Cu′ was fixed at a value approximately equal to U_{eq} for Cu. All H atoms were refined isotropically, and all other atoms were refined anisotropically. Depending on the refinement method (see above), the occupancies of Cu and Cu′ changed as outlined in Table 2, and the coordinates and displacement parameters for Cu′ changed noticeably. For example, the three different refinements gave Cu···Cu′ distances of 0.65–0.75 Å; this suggests that the esd values associated with Cu′ are unrealistically small. No other parameters changed by more than half of their estimated standard deviations in these refinements.

Figures 2 and 3 are ORTEP[22] drawings for the 195 and 110 K structures. Important distances and angles are listed in Table 3 and 4. Also included for comparison are values from our previous refinement using 296 K data[3] and from the 243 K structure reported by Hampden-Smith and co-workers.[12] Coordinates, displacement parameters, and peripheral distances and angles are available in the supplementary material (see paragraph at end of article).

(22) Johnson, C. K. *ORTEP-II: A Fortran Thermal-Ellipsoid Plot Program for Crystal-Structure Illustrations*; Report ORNL-5138; National Technical Information Service, U.S. Department of Commerce: Springfield, VA, 1976.

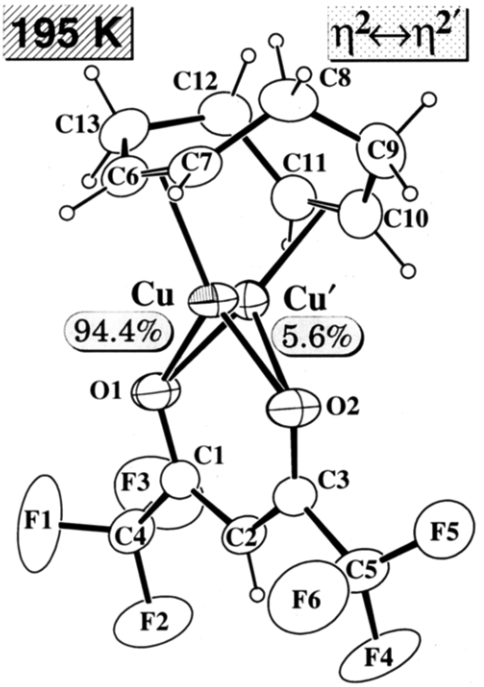

Figure 2. ORTEP[22] illustration of (hfac)Cu(COD) based on data collected at 195 K, with ellipsoids at the 50% probability level (H atoms shown as circles of arbitrary radius). Both Cu (foreground, one octant shaded) and Cu′ (no shading on ellipsoid) are shown. Boxes near Cu atoms indicate occupancies used in final refinement; see text for details.

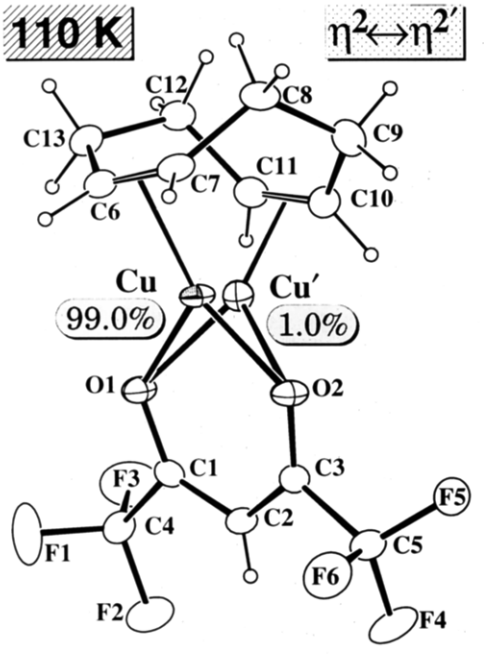

Figure 3. ORTEP[22] illustration of (hfac)Cu(COD), as in Figure 2 but based on data collected at 110 K.

Solid-State ^{13}C NMR Spectroscopy. Solid-state CP/MAS ^{13}C NMR spectra were obtained at 50.3 MHz (4.7 T) using a Bruker MSL200 spectrometer. Samples were loaded in a 7-mm ZrO_2 rotor with a Kel-F cap and spun at 4 kHz with dry nitrogen gas. Temperature was monitored by a copper–constantan thermocouple located near the MAS stator. The temperature control unit is accurate to within ±2 K based on comparison with a calibrated Pt resistance thermometer, and temperature control at the sample is estimated to be within ±5 K. Data acqusition was via a single-contact Hartmann–Hahn cross polarization pulse sequence.[23] The parameters used for most experiments were the following: 5-μs ^1H 90° pulse, 2-ms cross-polarization time, and 60-s recycle delay. Usually, 30–100 free induction decays were acquired and an exponential line-broadening factor of 20 Hz was applied. The ^{13}C chemical shift values were recorded on the δ scale indirectly referenced through adamantane (external reference) to TMS. One spectrum was acquired at 125.8 MHz (11.7 T) using a Bruker MSL500 spectrometer and a 4-mm ZrO_2 MAS rotor at a spin rate of 12 kHz. The possibility of sample decomposition during the 320 and 340 K NMR experiments was examined by acquiring room-temperature ^{13}C NMR spectra after each run; no significant changes were observed. Simulated line shapes (see the Results) were fitted to the observed spectra by eye, since the additional peaks in this spectral region would have made a least-squares or other mathematical fitting technique difficult.

Table 3. Important Distances in (hfac)Cu(COD) (angstroms)

distance	296 ± 2 K[a]	296 ± 2 K[b,c]	243 K[d]	195 ± 3 K[b]	110 ± 3 K[b]
Cu···Cu′	0.472(7)	0.614(7)		0.623(7)	0.70(3)
Cu–O1	2.001(4)	2.003(4)	1.999(6)	1.994(2)	1.996(1)
Cu–O2	1.995(4)	1.993(4)	2.001(4)	1.990(2)	1.992(1)
Cu–C6	2.013(5)	2.017(5)	2.049(6)	2.034(2)	2.041(2)
Cu–C7	2.056(5)	2.057(4)	2.089(7)	2.074(2)	2.076(2)
Cu···C10	2.508(5)	2.502(5)	2.466(8)	2.461(2)	2.446(2)
Cu···C11	2.590(5)	2.587(5)	2.550(7)	2.550(2)	2.535(2)
Cu–C67	1.918[e]	1.920	1.953	1.940	1.941
Cu···C1011	2.464	2.459	2.418	2.416	2.399
Cu′–O1	2.004(8)	2.018(9)		2.009(6)	2.05(2)
Cu′–O2	1.976(8)	2.000(9)		2.013(6)	1.96(3)
Cu′···C6	2.270(8)	2.362(8)		2.394(7)	2.50(3)
Cu′···C7	2.277(7)	2.366(8)		2.403(7)	2.47(3)
Cu′–C10	2.117(9)	2.007(9)		1.966(7)	1.90(3)
Cu′–C11	2.235(8)	2.131(9)		2.093(7)	2.08(3)
Cu′···C67	2.170	2.264		2.301	2.39
Cu′–C1011	2.076	1.963		1.918	1.88
C6═C7	1.356(6)	1.356(6)	1.367(11)	1.353(4)	1.371(3)
C10═C11	1.311(6)	1.311(6)	1.331(10)	1.332(3)	1.342(3)

[a] Reference 3. [b] This work. [c] Alternate refinement of data from ref 3 (see text for details). [d] Reference 12. [e] Distances involving the calculated centroids C67 and C1011 are given without estimated standard deviations.

Results

Crystal-Structure Determinations. Unit-cell dimensions for (hfac)Cu(COD) show no abrupt changes with temperature; all three axis lengths and β decrease at lower temperatures. We carried out the low-temperature measurements in order to evaluate the model we proposed previously, namely, that the Cu and Cu′ sites were involved in η^2 and η^4 coordination respectively to the COD ligand.[3] Hampden-Smith and co-workers had reported a structure determination with data collected at 243 K.[12] However, although they observed a difference Fourier peak of height 1.7 e Å^{-3}, 0.99 Å from the Cu atom, they did not include a second Cu atom in their model.

For the present work, we first collected diffraction data at 110 K, in order to obtain higher-resolution data to determine the position of Cu′ more accurately. The results we obtained at this temperature clearly indicate that nearly all of the electron density associated with the copper atom is at the Cu site (η^2). Cu′ is not precisely located, because it corresponds to a very small amount of electron density, but it appears also to be in an η^2 position (much closer to C10═C11 than to C6═C7).

Because the results of the 110 K refinement were not conclusive, we decided to collect data at an intermediate temperature (195 K), where Cu′ might be both well resolved and adequately populated. These results were more

(23) Gerstein, B. C.; Dybowski, C. R. *Transient Techniques in NMR of Solids*; Academic Press: New York, 1985.

conclusive, strongly supporting the model of two η^2 sites for the copper atom. Approximately 6% of the copper electron density is at the Cu′ site (see Experimental Section), and this proved to be enough for accurate resolution and refinement of both sites.

Rerefinement of Room-Temperature Data. We initially attempted a new refinement using our previous 296 K data set because we noticed that the equivalent isotropic displacement parameter U_{eq} for Cu′ in our first model[3] was approximately twice as large as that for Cu. This was surprising, because one ordinarily expects refined displacement parameters for identical atoms to be similar. This disparity in U_{eq} could have arisen if we had overestimated the occupancy of Cu′. Therefore, we carried out a new refinement (via damped least-squares analysis), allowing occupancy and anisotropic displacement parameters to vary for both Cu and Cu′.

Two features of the new room-temperature model are of interest. First, the occupancies of Cu and Cu′ converged to somewhat higher (77.7%) and lower (22.3%) values respectively. (The new values of U_{eq} for Cu and Cu′ are somewhat closer, but they still differ substantially. The remaining differences may represent genuine differences in thermal motion at the two sites, or they may reflect uncertainities caused by the poor resolution of the sites at room temperature.) Second, the Cu and Cu′ positions are approximately 0.14 Å farther apart in the new refinement than in our original model, and the new position for Cu′ is substantially closer to C10=C11 than to C6=C7. That is, the newly refined model using data collected at room temperature suggests disorder between two η^2 structures rather than between η^2 and η^4 structures.

Thus, the results of refinement using the room-temperature data depend significantly on the model chosen, but they are not inconsistent with two contributing η^2 structures. The low-temperature results, on the other hand (especially those from 195 K), strongly support the model of two η^2 structures.

Solid-State NMR Data. The ^{13}C CP/MAS spectrum at 190 K, presented in Figure 4, shows resonances due to the carbonyl of the hfac ligand ($CF_3\underline{C}O$–, 178 ppm), the methylenes (–$\underline{C}H_2$–, 28 ppm) and methines (—$\underline{C}H$=, 127 and 105 ppm) of the COD ligand, the $\underline{C}F_3$ groups (118 ppm), and the methine site in the hfac ligand (H-$\underline{C}(COCF_3)_2$, weak, broad resonance at 88 ppm). Chemical shifts and assignments are summarized in Table 5.

We attribute the two ^{13}C resonances at 127 and 105 ppm to the free and bound olefinic carbons, respectively, of an η^2-COD ligand. These assignments are based on olefinic ^{13}C chemical shifts in the following closely related compounds: COD, 129 ppm; (hfac)Cu^I(η^2-cyclooctene), 102 ppm (in CD_2Cl_2). Solutions of (hfac)Cu^I(COD) show a single resonance at 114.1 ppm which is unsplit in solution even at ca. 200 K; this has been attributed to rapid exchange between free and bound COD.[3,12]

The large line width for the methine site is attributed to ^{13}C–^{19}F dipolar coupling. The CF_3 resonance is easily observed in spite of potential ^{13}C–^{19}F dipolar coupling; apparently, the dipolar coupling is motionally averaged to near zero by rapid CF_3 group rotation. (This type of rotation could easily account for the disorder observed in the CF_3 groups in the room-temperature X-ray analysis. Our model for the CF_3 groups in the 195 K structure included only one set of F atoms. Still, their displacement parameters refined to large values, and many of the most intense peaks in the final difference Fourier map were within bonding distance of the CF_3 carbon atoms. Thus, the CF_3 groups are probably disordered at 195 K as well as at room temperature, possibly due to continued rapid rotation; this is consistent with negligible ^{13}C–^{19}F dipolar coupling.)

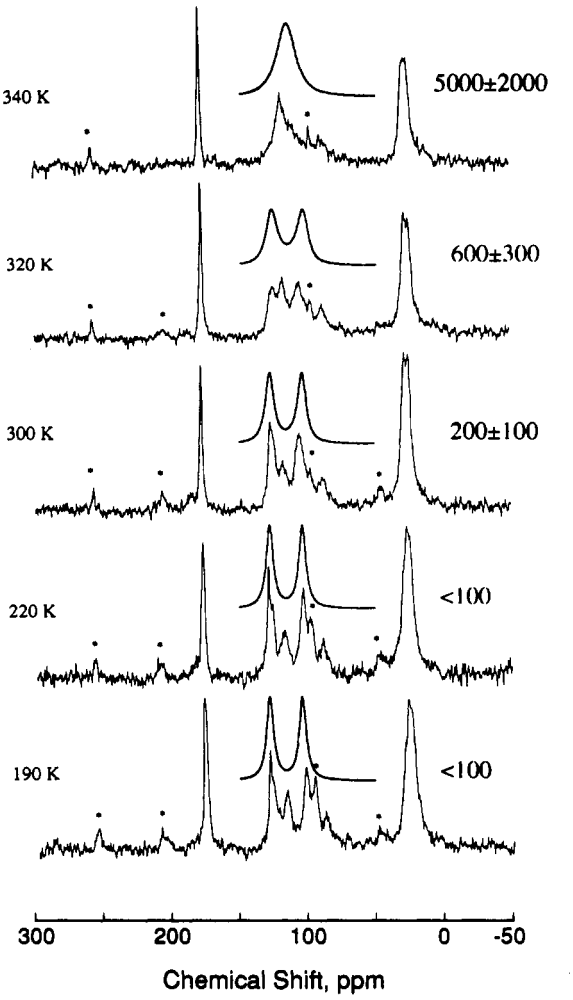

Figure 4. Solid-state ^{13}C CP/MAS NMR spectra at 4.7 T of (hfac)Cu(COD) as a function of temperature. After each spectrum acquired at 320 and 340 K, a spectrum was acquired at ca. 300 K to check for sample decomposition; none was detected. Spinning sidebands are labeled with asterisks. Above each spectrum is a trace from a simulation of a two-site chemical exchange; at the side are the exchange rates (in s^{-1}) used in the simulations. T_2 is set to 1 ms.

We were also concerned that line shapes for ^{13}C sites near the $^{63/65}Cu$ nuclei might be complicated by a second-order quadrupole effect transmitted via dipolar or scalar coupling.[24-27] For example, the ^{31}P CP/MAS NMR spectrum of bis(triphenylphosphine)copper(I) nitrate shows a three-line pattern at 1.4 T and a four-line pattern at 7 T.[24] When the $^{63/65}Cu$ quadrupole interaction exceeds the $^{63/65}Cu$ Zeeman interaction, second-order quadrupole effects can become important. A second requirement is a significant dipolar or scalar interaction between the ^{13}C and $^{63/65}Cu$ sites. For (hfac)Cu^I(COD), the dipolar cou-

(24) Menger, E. M.; Veeman, W. S. *J. Magn. Reson.* **1982**, *46*, 257.
(25) Naito, A.; Ganapathy, S.; McDowell, C. A. *J. Magn. Reson.* **1982**, *48*, 367.
(26) Böhm, J.; Frenzke, D.; Pfeifer, H. *J. Magn. Reson.* **1983**, *55*, 197.
(27) Gobetto, R.; Harris, R. K.; Apperley, D. C. *J. Magn. Reson.* **1992**, *96*, 119.

Table 4. Angles Involving Cu Atoms in (hfac)Cu(COD) (degrees)

angle	296 ± 2 K[a]	296 ± 2 K[b,c]	243 K[d]	195 ± 3 K[b]	110 ± 3 K[b]
O1-Cu-O2	93.1(2)	93.1(1)	93.3(2)	93.47(6)	94.02(5)
O1-Cu-C6	110.0(2)	109.8(2)	108.5(3)	108.70(8)	107.86(7)
O1-Cu-C7	148.6(2)	148.3(2)	146.5(2)	146.76(9)	146.40(7)
O1-Cu···C10	111.8(2)	112.0(2)	113.8(2)	112.53(8)	112.35(6)
O1-Cu···C11	92.4(2)	92.4(1)	93.4(2)	92.21(8)	91.57(6)
O1-Cu-C67	129.6[e]	129.3	127.8	127.97	127.35
O1-Cu···C1011	102.2	102.3	103.7	102.44	102.03
O2-Cu-C6	151.3(2)	151.3(2)	149.8(3)	150.31(8)	149.86(7)
O2-Cu-C7	115.5(2)	115.6(2)	115.4(2)	115.86(8)	115.40(7)
O2-Cu···C10	92.4(2)	92.7(2)	94.0(2)	93.58(8)	93.93(6)
O2-Cu···C11	116.8(2)	117.1(2)	119.3(2)	118.88(8)	119.66(6)
O2-Cu-C67	133.7	133.7	133.0	133.52	133.16
O2-Cu···C1011	105.0	105.3	107.1	106.66	107.24
C6-Cu-C7	38.9(2)	38.9(2)	38.6(3)	38.4(1)	38.90(8)
C6-Cu···C10	94.4(2)	94.5(2)	95.7(3)	95.72(9)	96.47(7)
C6-Cu···C11	80.1(2)	80.1(2)	80.8(3)	80.72(9)	81.09(7)
C7-Cu···C10	81.2(2)	81.3(2)	82.5(3)	82.43(9)	82.88(7)
C7-Cu···C11	86.2(2)	86.3(2)	87.4(3)	87.11(9)	87.68(7)
C10···Cu···C11	29.7(1)	29.8(1)	30.7(2)	30.76(8)	31.20(6)
C67-Cu···C1011	85.0	85.1	86.2	86.09	86.67
O1-Cu′-O2	93.6(3)	92.4(3)		92.3(3)	93(1)
O1-Cu′···C6	100.4(4)	97.0(3)		95.7(3)	91(1)
O1-Cu′···C7	131.5(4)	125.8(4)		123.9(3)	119(1)
O1-Cu′-C10	130.6(4)	136.9(4)		138.3(4)	139(2)
O1-Cu′-C11	103.8(4)	107.1(4)		107.0(3)	105(1)
O1-Cu′···C67	116.2	111.6		110.0	105
O1-Cu′-C1011	117.4	122.2		122.8	121
O2-Cu′···C6	132.2(4)	125.7(4)		123.7(3)	121(1)
O2-Cu′···C7	107.1(3)	103.1(3)		102.2(3)	101(1)
O2-Cu′-C10	106.0(4)	109.4(4)		110.1(3)	115(1)
O2-Cu′-C11	137.0(4)	143.2(4)		145.4(4)	152(2)
O2-Cu′···C67	120.4	115.0		113.5	112
O2-Cu′-C1011	122.3	127.2		128.7	135
C6···Cu′···C7	34.7(2)	33.3(2)		32.8(1)	32.0(4)
C6···Cu′-C10	98.8(3)	99.1(4)		99.8(3)	98(1)
C6···Cu′-C11	83.3(3)	83.4(3)		83.5(2)	81.0(8)
C7···Cu′-C10	85.6(3)	85.8(3)		86.2(2)	85.8(9)
C7···Cu′-C11	90.3(3)	90.6(3)		90.7(2)	89.2(9)
C10-Cu′-C11	34.9(2)	36.8(2)		38.1(2)	39.0(5)
C67···Cu′-C1011	89.4	89.6		89.9	88
Cu-O1-C1	122.8(3)	122.8(3)	122.6(5)	122.7(1)	122.1(1)
Cu′-O1-C1	119.6(3)	118.4(3)		117.6(2)	114.3(7)
Cu-O2-C3	122.3(3)	122.4(3)	122.4(5)	122.9(1)	122.4(1)
Cu′-O2-C3	119.7(3)	118.2(3)		117.8(2)	116.9(8)
Cu-C6-C7	72.2(3)	72.1(3)	72.3(4)	72.4(1)	71.9(1)
Cu-C6-C13	109.5(3)	109.4(3)	107.6(4)	108.6(2)	108.1(1)
Cu′···C6-C7	72.9(3)	73.5(3)		74.0(2)	72.6(6)
Cu′···C6-C13	100.6(3)	98.0(3)		97.1(2)	97.0(6)
Cu-C7-C6	68.9(3)	69.0(3)	69.1(4)	69.2(1)	69.2(1)
Cu-C7-C8	113.8(3)	113.6(3)	111.7(4)	112.6(2)	112.0(1)
Cu′···C7-C6	72.4(3)	73.2(3)		73.3(2)	75.4(6)
Cu′···C7-C8	103.0(3)	100.3(3)		99.5(2)	97.4(7)
Cu···C10-C9	95.8(3)	95.8(3)	96.5(5)	96.0(2)	96.3(1)
Cu···C10-C11	78.6(3)	78.7(3)	78.1(5)	78.3(1)	78.0(1)
Cu′-C10-C9	101.7(4)	104.3(4)		105.1(3)	106.0(8)
Cu′-C10-C11	77.4(4)	76.7(4)		76.1(2)	77.8(8)
Cu···C11-C10	71.6(3)	71.5(3)	71.1(4)	70.9(1)	70.8(1)
Cu···C11-C12	100.2(3)	100.3(3)	100.6(4)	101.0(1)	101.9(1)
Cu′-C11-C10	67.6(3)	66.5(4)		65.7(2)	63.2(7)
Cu′-C11-C12	107.6(3)	110.4(4)		111.5(2)	115.3(8)

[a] Reference 3. [b] This work. [c] Alternate refinement of data from ref 3 (see text for details). [d] Reference 12. [e] Angles involving the calculated centroids C67 and C1011 are given without estimated standard deviations.

Table 5. ^{13}C NMR Data

		δ/ppm vs TMS				
sample	medium	$-\underline{C}H_2-$	$-\underline{C}H=$	$-\underline{C}F_3$	$-\underline{C}O-$	$-\underline{C}H(CO)_2$
COD	CD_2Cl_2	28.4	129.0			
(hfac)Cu(COD)	CD_2Cl_2	28.6	114.1	118.6	177.8	89.0
(hfac)Cu(COD)	solid	28	127, 105	118	177	88

pling constant is relatively small; d(C–Cu) = 2.05 Å yields a value of 929 Hz. If the ^{63}Cu quadrupole coupling constant has a typical magnitude of 30 MHz,[28] then a multiplet covering a range of 15 ppm would be expected at a field of 4.7 T. This is, however, an upper bound, as the actual magnitude of the ^{63}Cu quadrupole coupling constant may be significantly smaller. One observation indicating a negligible second-order quadrupole effect in (hfac)Cu^{I}(COD) is its ^{13}C CP/MAS spectrum at 300 K and 11.7 T. If the 4.7-T spectrum was dominated by a second-order quadrupole effect, then the 11.7-T spectrum should be less complex due to the larger $^{63/65}Cu$ Zeeman interaction. The COD olefin resonances at 300 K and 11.7 T are nearly identical to those observed at 190 K and 4.7 T, indicating

(28) See, for example: Negita, H.; Hiura, M.; Yamada, K.; Okuda, T. *J. Mol. Struct.* **1980**, *58*, 205.

that quadrupole effects are nugatory in the lower-field spectrum. (We also searched for second-order quadrupole effects in the 4.7-T ^{13}C CP/MAS NMR spectra of three other metal–olefin complexes. No significant effects were observed, as judged by their relatively narrow ^{13}C —*C*H= resonances: $PdCl_2(\eta^4$-COD), 203-Hz fwhm; $[CuCl(\eta^2$-NBD)]$_4$, 632 Hz; $[Cu(\eta^4$-COD)]$_2(\mu$-Cl)$_2$, 322 Hz.)

The exchange-broadened line shapes for the COD olefin carbon resonances were modeled using modified Bloch equations for two-site exchange.[29] Interestingly, even though the populations of the Cu and Cu′ sites vary with temperature, the total populations of free and bound olefins ($\delta(^{13}C)$ 127 and 105 ppm, respectively) remain equal at all temperatures. Thus, the simple two-site model with equal populations is appropriate. The results of the NMR line-shape calculations, including estimated exchange rates, are shown in Figure 4.

Discussion

Geometry of the Complex. The coordination environment at Cu has been described as "3+1",[12] i.e., essentially trigonal planar, but with C10=C11 a distant fourth ligand. The arrangement of O1, O2, and the C10=C11 centroid about Cu′ is similar, with C6=C7 also considerably farther away. (Our original refinement using room-temperature data placed Cu′ in a more symmetrical η^4 site, between C6=C7 and C10=C11. However, as mentioned above, our rerefinement using the room-temperature data, and the two low-temperature models, all support the picture of two η^2-bound Cu sites.) C6=C7 is significantly longer than C10=C11 in all models. This is to be expected because, in all of the models, the Cu atom is coordinated to C6=C7 more often than to C10=C11.

The individual distances in the complex are within normal ranges. The Cu–O distances, 1.99–2.00 Å, in the present structure are similar to those found in related three-coordinate hfac–Cu(I) complexes: (hfac)Cu(tmvs) (1.95 Å),[7] [(hfac)Cu]$_2(\mu$-COT) (1.92–2.09 Å),[2] and (hfac)-Cu(PCy$_3$) (1.99–2.03 Å).[11] (The only genuine four-coordinate hfac-Cu complex to have been studied crystallographically, (hfac)Cu(PCy$_3$)$_2$,[11] shows significantly longer Cu–O distances, 2.21–2.25 Å; however, this elongation may be due primarily to the presence of two very bulky PCy$_3$ ligands.) Cu–O distances in hfac–copper(II) complexes are generally slightly smaller (1.91–1.97 Å).[30]

The conformation of the COD ligand is the twist-boat of approximate 2-fold symmetry. Deviations from exact C_2 symmetry are small, and no significant differences are observed among the three different temperatures of our study. Using our 110 K model, for which the uncertainties in torsion angles are smallest, the asymmetry parameter ΔC_2[31] has a value of only 3.5°, and the largest single difference for "C_2-related" torsion angles is 5.3(4)°. A very similar conformation was found for 1,5-COD by gas-phase electron diffraction and predicted by molecular mechanics calculations.[32] Endocyclic torsion angles for the structures discussed here are given in the supplementary material.

The range of Cu–C distances reported in copper(I)–olefin complexes is broad, 1.94–2.22 Å.[2,19,20,33] Still, despite the "softness" of this interaction, it is clear that the Cu–C distances in the present work (i.e., the revised model for the room-temperature data and both low-temperature structures) represent exclusively the η^2 coordination mode for the COD ligand.

Energetics. In the crystal, the copper atom is coordinated predominantly to C6=C7 at all temperatures studied. We attribute this preference to the asymmetric orientation of Cu and Cu′, and the two olefinic double bonds, relative to the hfac moiety. For example, using the data from the 195 K structure, C1, C2, C3, O1, and O2 are planar within 0.008(2) Å. The deviations of other atoms from this plane are as follows: Cu, −0.079(1); C6, 0.483(2); C7, 0.329(2); C67, 0.406; Cu′, −0.683(5); C10, −2.385(2), C11, −2.355(2); C1011, −2.370 Å. Thus, a copper atom at the Cu site can be nearly coplanar with both the hfac and olefin ligands, whereas binding at the Cu′ site requires significant deviation from planarity.

The population ratios obtained in the X-ray analyses may be treated as equilibrium constants for the "reaction" Cu ↔ Cu′ and then converted to ΔG values; see Table 2. The few data points preclude detailed analysis, but the calculated ΔG values are consistent with a slightly endothermic reaction, with ΔS close to zero.

There are several possible explanations for the fact that the calculated ΔG values do not show a consistent trend with temperature. Perhaps the most likely is that the refined populations at 110 K are incorrect. When the occupancy of Cu′ is small, even a small error in estimating it would result in a large error in ΔG. It is often difficult to locate small atoms (such as H) accurately when they are near transition metals; the present structure, with ca. 1% of the copper atom at a second nearby site, poses a similar problem. Also, even our largest set of data (at 195 K, with θ_{max} = 38°) gives a theoretical optimum resolution of ca. 0.58 Å, only slightly smaller than the refined Cu···Cu′ distances. (This situation is unlikely to be improved by higher-resolution X-ray data, since the two Cu sites are separated by less than the ionic radius of Cu^+, 0.77 Å.[34]) Finally, we found that the refined populations vary significantly depending on the model chosen; this suggests that the populations are not highly reliable. In related work, Parkin et al. studied disorder between O and Cl atoms in molybdenum–phosphine complexes:[35] Refined occupancies from X-ray data showed the correct trends in population ratios but did not always reproduce known compositions quantitatively.

Other investigators have studied crystallographic disorder attributable to chemical reactions (including rearrangements and isomerizations) in the solid state. Several

(29) Sandström, J. *Dynamic NMR Spectroscopy*; Academic Press: New York, 1982.
(30) Belford, R. C. E.; Fenton, D. E.; Truter, M. R. *J. Chem. Soc., Dalton Trans.* **1974**, 17. Belford, R. C. E.; Fenton, D. E.; Truter, M. R. *J. Chem. Soc., Dalton Trans.* **1972**, 2208. Durley, R. C. E.; Fenton, D. E.; Truter, M. R. *Acta Crystallogr., Sect. B* **1980**, *36B*, 2991. Dickman, M. H.; Doedens, R. J. *Inorg. Chem.* **1981**, *20*, 2677. Gatteschi, D.; Laugier, J.; Rey, P.; Zanchini, C. *Inorg. Chem.* **1987**, *26*, 938.
(31) Duax, W. L.; Norton, D. A. *Atlas of Steroid Structure*; Plenum: New York, 1975; Vol. 1.
(32) Hagen, K.; Hedberg, L.; Hedberg, K. *J. Phys. Chem.* **1982**, *86*, 117 and references therein.
(33) Baenziger, N. C.; Richards, G. F.; Doyle, J. R. *Inorg. Chem.* **1964**, *3*, 1529. Masuda, H.; Yamamoto, N.; Taga, T.; Machida, K.; Kitagawa, S.; Munakata, M. *J. Organomet. Chem.* **1987**, *322*, 121. Turner, R. W.; Amma, E. L. *J. Am. Chem. Soc.* **1963**, *85*, 4046; **1966**, *88*, 1877. Thompson, J. S.; Harlow, R. L.; Whitney, J. F. *J. Am. Chem. Soc.* **1983**, *105*, 3522. Ganis, P.; Lepore, U.; Paiaro, G. *J. Chem. Soc. D* **1969**, 1054. Cu–(C=C centroid) distances in [(hfac)Cu]$_2(\mu$-COT) are in the range 1.90–1.94 Å.[2b]
(34) Shannon, R. D. *Acta Crystallogr., Sect. A* **1976**, *A32*, 751.
(35) Yoon, K.; Parkin, G. *J. Am. Chem. Soc.* **1992**, *114*, 2210. Yoon, K.; Parkin, G.; Rheingold, A. L. *J. Am. Chem. Soc.* **1991**, *113*, 1438.

such systems involve crystallographically equivalent positions, so that the populations of the two sites are constrained to be equal at all temperatures. These include beryllocene, whose Be atoms are disordered between η^1 and η^5 coordination to the cyclopentadienyl groups,[36] and naphthazarin B, which shows a similar disorder involving localization of hydrogen-bonded H atoms.[13] In other cases, low-temperature X-ray data have been used to measure population differences between chemically and crystallographically inequivalent sites. Good examples of this phenomenon include the high-spin ↔ low-spin interconversion of $Fe(amp)_3Cl_2 \cdot CH_3OH$[37] and the equilibrium between five- and six-coordinate forms of $Fe^{III}TPP(PhS)(PhSH)$.[38] The present system is unusual in that although the two contributing forms have the same connectivity, they are not crystallographically equivalent. As a result, their energies are not necessarily equal, and their relative populations may depend on temperature.[39]

Dynamics. In addition to the information concerning energy differences between the Cu and Cu′ sites obtained from the X-ray data, the NMR spectra can be interpreted in terms of the rate of interconversion between Cu and Cu′. We have discussed above how the lineshapes were fit at each temperature. Only at ≥300 K is there strong evidence for exchange broadening; thus, only data from the three highest temperatures can be used to estimate exchange rates.

We used the Eyring equation $\Delta G^{\ddagger} = -RT\ln(\kappa hk/(k_B T))$[40] to obtain the free energies of activation $\Delta G^{\ddagger}$ given in Table 2. No clear trend in $\Delta G^{\ddagger}$ with temperature was evident; this suggests that $\Delta S^{\ddagger}$ is close to zero and $\Delta H^{\ddagger}$ is ca. 60 kJ mol^{-1}.[41] Data over a larger temperature or magnetic-field range might have enabled us to discern trends in $\Delta G^{\ddagger}$ more easily. However, neither lower temperatures (where all spectra appear to be in the slow-exchange limit) nor higher temperatures (approaching the fast-exchange limit) would be likely to be useful. The other solid-state spectrometer used in this work (11.7 T) would lead to measurable exchange only at *higher* temperatures, where volatility and decomposition of the complex are expected to cause serious problems.

Relation to CVD. The X-ray and NMR data for the present system give us information concerning both energy differences (ΔG) and interconversion barriers ($\Delta G^{\ddagger}$) for the process Cu ↔ Cu′. Thus, we can propose a free-energy diagram for the interconversion, which we have superimposed on a stick figure of (hfac)Cu(COD) in Figure 1. The Cu and Cu′ sites have stabilities that differ by only a few kJ mol^{-1}, but with a substantial barrier (ca. 60 kJ mol^{-1}) separating them.

The interconversion between Cu and Cu′ involves breaking one Cu–olefin bond and forming another. The transition state for the interconversion must involve substantial bond breaking, and we propose that its energy is an indication of the Cu–olefin bond dissociation energy. (The transition state is likely to involve approximately equal bonding between Cu and the two double bonds; thus, it has some (hfac)Cu(η^4-COD) character. However, the two bonds in this "η^4" transition state must be much weaker than the ideal Cu–olefin bond.) Figure 5 is a "two-dimensional" interpretation of the potential-energy surface for this system. According to this diagram, the Cu ↔ Cu′ interconversion is a way of "trapping" the COD ligand after partial dissociation has occurred; thus, the compound offers an approach to the bond dissociation energy in a reversible fashion.

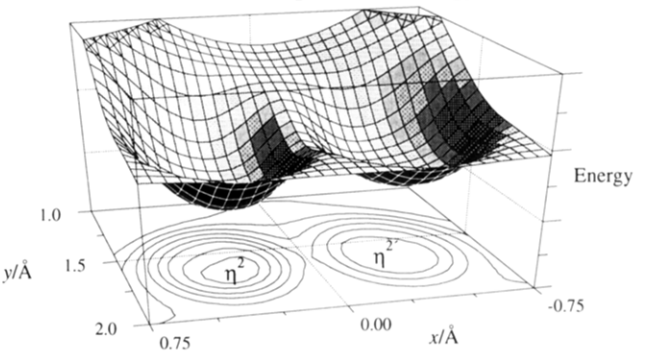

Figure 5. Proposed potential-energy surface for (hfac)Cu(COD) as a function of position of the (hfac)Cu moiety relative to the COD ligand. The two potential wells, which correspond to the Cu (η^2) and Cu′ ($\eta^{2'}$) positions, are ca. 0.6 Å apart and differ in energy by 3–5 kJ mol^{-1}. (The coordinates of the double-bond centroids "C67" and "C1011", using the x and y axes drawn here, are approximately (±1.5, 0).) The barrier connecting Cu and Cu′ is ca. 60 kJ mol^{-1} in height, but this is smaller than the amount of energy required for complete dissociation of the COD ligand.

The experiments most closely related to the present work appear to be those of Dubois and Zegarski,[9] who examined the dissociation of neutral ligands from (hfac)Cu^I complexes adsorbed on copper surfaces. Their temperature-programmed-desorption (TPD) data yielded an activation energy of 59 kJ mol^{-1} for the loss of COD(g) from (hfac)Cu(COD) adsorbed on Cu(100); this is very close to the height we observe for the Cu ↔ Cu′ interconversion barrier. This value is also close to those reported for desorption of ethylene from copper surfaces.[17]

All of the barriers for these Cu-based systems are considerably smaller than metal–olefin bond energies for other metals.[42] This is consistent with the low activity of Cu for catalytic processes such as the hydrogenation of ethylene.[43] (A still smaller barrier, 25 ± 5 kJ mol^{-1}, was measured for dissociation of the gaseous Cu–C_2H_4 complex.[44] Thus, the interaction of an olefin with a single copper atom appears to be weak, but it is stronger to a Cu surface or to a Cu(I) complex.[45])

(36) Nugent, K. W.; Beattie, J. K.; Hambley, T. W.; Snow, M. R. *Aust. J. Chem.* **1984**, *37*, 1601.
(37) Katz, B. A.; Strouse, C. E. *J. Am. Chem. Soc.* **1979**, *101*, 6214.
(38) Collman, J. P.; Sorrell, T. N.; Hodgson, K. O.; Kulshrestha, A. K.; Strouse, C. E. *J. Am. Chem. Soc.* **1977**, *99*, 5180.
(39) Doyle and co-workers[2b] also refined the occupancies of the disordered Cu atoms in [(hfac)Cu]$_2$(μ-COT), obtaining population ratios of 0.67:0.33 and 0.55:0.45 for the two independent Cu sites in the molecule. However, the [(hfac)Cu]$_2$(μ-COT) X-ray data were collected only at room temperature.
(40) Glasstone, S.; Laidler, K. J.; Eyring, H. *The Theory of Rate Processes*; McGraw-Hill: New York, 1941; p 195. We assumed unit transmission coefficient κ in our work.
(41) An Arrhenius plot, i.e., a fit to $\ln k = A\exp(-E_a/RT)$, gave E_a = 68 kJ mol^{-1}. Since $E_a = \Delta H^{\ddagger} + RT$ for unimolecular reactions,[40] this result is approximately consistent with our analysis of $\Delta G^{\ddagger}$.
(42) 112 and 108 kJ mol^{-1} for each Mo–olefin bond in Mo(CO)$_4$(η^4-norbornadiene) and Mo(CO)$_4$(η^4-COD), respectively: Mukerjee, S. L.; Nolan, S. P.; Hoff, C. D.; Lopez de la Vega, R. *Inorg. Chem.* **1988**, *27*, 81. 130 kJ mol^{-1} for dissociation of the first ethylene ligand in $CpRh(C_2H_4)_2$: Cramer, R. *J. Am. Chem. Soc.* **1972**, *94*, 5681.
(43) Bond, G. C. *Heterogeneous Catalysis: Principles and Applications*; Clarendon: Oxford, England, 1987; p 65. For further studies of the strength of the Cu–olefin bond, see: Nyberg, C.; Tengstål, C. G.; Andersson, S.; Holmes, M. W. *Chem. Phys. Lett.* **1982**, *87*, 87. Demuth, J. E. *IBM J. Res. Dev.* **1978**, *22*, 265.
(44) Blitz, M. A.; Mitchell, S. A.; Hackett, P. A. *J. Phys. Chem.* **1991**, *95*, 8719.

Our barrier is also substantially smaller than the experimental activation energies observed for Cu CVD using (hfac)Cu(COD) as precursor (109[5] or 125 kJ mol^{-1} [6]). However, since the rate-limiting steps in these CVD processes have not been identified with certainty,[46] their activation energies represent only upper limits for the Cu–olefin bond dissociation energy. Therefore, the TPD experiments are most closely related to the dynamic process we observe in crystalline (hfac)Cu(COD).

Summary

We have studied bonding, energetics, and dynamics in the solid CVD precursor (hfac)Cu(COD), by means of X-ray structure analysis and solid-state ^{13}C NMR spectroscopy. This approach gives new insight into molecular rearrangement in this precursor, and we believe the new information is closely related to elementary steps in the CVD process.

Acknowledgment. We thank Dr. Robert Taylor of Bruker Instruments, Inc. for acquiring the 11.7-T ^{13}C NMR spectrum and Professor Gregory L. Griffin for numerous helpful discussions. This work was supported in part by the National Science Foundation (Grant CTS-9311527). R. K. is grateful for support through a joint research agreement between IBM Corp. and Louisiana State University. The purchase of the Bruker MSL200 NMR spectrometer was made possible by NSF Grant CHE-8711788.

Supplementary Material Available: Tables of atomic coordinates, peripheral distances and angles, anisotropic displacement parameters, and selected torsion angles (13 pages); a listing of calculated and observed structure factors (22 pages). Ordering information is given on any current masthead page.

(45) Ethylene is also more strongly bound (dissociation energy >85 kJ mol^{-1}) to Cu_2(g): Lian, L.; Akhtar, F.; Hackett, P. A.; Rayner, D. M. *Chem. Phys. Lett.* **1993**, *205*, 487.

(46) For a discussion of mechanistic steps in Cu CVD using (hfac)-Cu(tmvs) as precursor, see: Jain, A.; Chi, K. M.; Kodas, T. T.; Hampden-Smith, M. J.; Paffett, M. F.; Farr, J. D. *J. Electrochem. Soc.* **1993**, *140*, 1434.